Pure appl. geophys. 162 (2005) 1747–1778
0033–4553/05/101747–32
DOI 10.1007/s00024-005-2691-x

Pure and Applied Geophysics

Characteristics of Stable Flows over Southern Greenland

Andrew Orr,[1] Edward Hanna,[2] Julian C. R. Hunt,[1] John Cappelen,[3] Konrad Steffen,[4] and Ag Stephens[5]

Abstract — The main characteristic features of stable atmospheric flows over a large mountain plateau are summarised and then compared with mesoscale and synoptic scale numerical simulation, meteorological analysis, satellite imagery, and surface observations for the cases of flows over Southern Greenland for four wind directions. The detailed features are identified using the concepts and scaling of stably stratified flow over large mountains with variations in surface roughness, elevation, and heating. For westerly and easterly winds detached jets form at the southern tip, where coastal jets converge, which propagate large distances across the ocean. Near coasts katabatic winds can combine with barrier jets and wake flows generated by synoptic winds. Note how the approach flow rises/falls over southern Greenland for easterly/westerly winds, leading in both cases to more cloud on the western side. Some conclusions are drawn about the large-scale influences of these flows; detached jets in the atmosphere; air-sea interaction; formation of low pressure systems. For accurate simulations of these flows, mesoscale models are necessary with resolutions of order of 20 km or less.

Key words: Greenland, Wind-jets, Air-sea interaction, Synoptic flows.

1. Introduction

Greenland's vast size, remoteness, and inhospitable climate, mean meteorologically it is one of the least studied areas on Earth, especially on the mesoscale (10–100 km) (Putnins, 1970; Scorer, 1988). This is despite it being the largest ice-capped structure in the Northern Hemisphere (see Fig. 1). It is known that Greenland greatly influences the climate of northwest Europe as cold, stable air from the Arctic Ocean and the predominantly westerly flow across the North Atlantic is partially blocked (Scorer, 1988). Greenland is critically sensitive to climate change (e.g., Hanna and Cappelen, 2003). It is very sensitive to air-sea-ice coupling effects which have a

[1] Centre for Polar Observation and Modelling, Dept. of Space and Climate Physics, University College London, UK. Present affiliation: ECMWF, Shinfield Pk, Reading, UK
[2] Department of Geography, University of Sheffield, UK.
[3] Danish Meteorological Institute, Copenhagen, Denmark.
[4] Cooperative Institute for Research in Environmental Sciences, University of Colorado, U.S.A.
[5] British Atmospheric Data Centre, Rutherford Appleton Laboratory, UK.

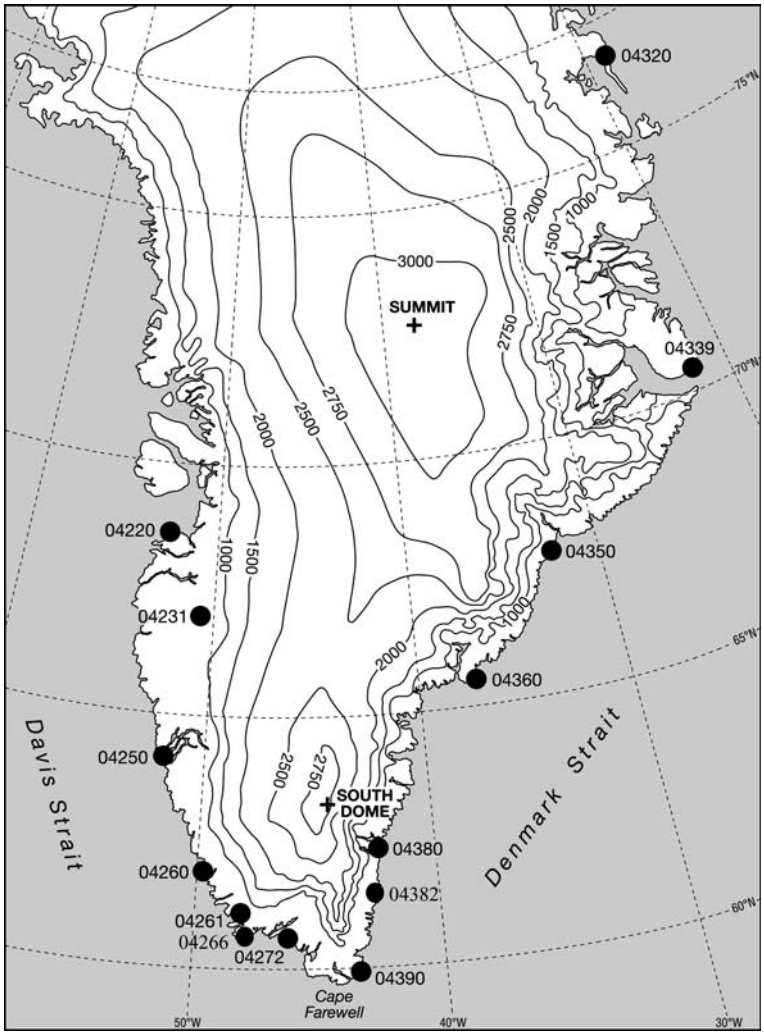

Figure 1
Map of southern Greenland showing orography elevation contours (in meters) and locations of the DMI and GC-Net stations used in this study.

marked effect on seasonal weather variations in northwest Europe (COLEMAN and DAVEY, 1999). For example, it acts as a large atmospheric heat sink through ice albedo feedback. And katabatic winds which flow from the broad gently sloping interior to the steep coastal margins are important to the energy balance of melting ice in the ablation zone during summer (MEESTERS, 1994).

The atmospheric flows and processes over Greenland occur on many length scales, from the microscale, to the mesoscale, to synoptic scales. Flow over and

around Greenland is affected by (i) the large and initially very steep elevation change between the coastal margins and the central plateau (~3 km; see Fig. 1), (ii) the combination of very rough surfaces (roughness length $z_0 \sim 1 - 10$ m) and jagged mountains around the coasts, (iii) the strong katabatic flows from the plateau down to the coasts (~ 100 km) (BROMWICH *et al.*, 1996; KLEIN and HEINEMANN, 2002), (iv) the presence of fjords, such as Kangerlussuaq and Sermilik located in the southwest coastal margins (RASMUSSEN, 1989; KLEIN *et al.*, 2001), (v) the presence of the semi-permanent Icelandic Low (~ 1000 km) (SCORER, 1988), (vi) air-sea-ice interaction processes (STAMMERJOHN *et al.*, 2003), and (vii) associated boundary layer processes (SMEDMAN *et al.*, 2003). Here there are extremely sharp gradients in roughness and elevation. These result in local scale phenomena that have long been observed, for example, coastal wind jets, but as they occur on kilometre length scales, they are only described by numerical mesoscale models when they are run with fine resolution (e.g., CAPON, 2003). A high spatial resolution is also required to adequately resolve the steep orography near the coast (GLOVER, 1999). These local scale phenomena can have large-scale climate effects, e.g. drag, wind waves, downwelling, cyclogenesis, air-sea-ice interaction, etc.

To help define the magnitudes and spatial and temporal scales of these types of stable, mesoscale flows, HUNT *et al.*, (2001) applied a general linearised perturbation model to atmospheric flows over large mountains, in order to predict the overall flow, particularly deflection, waves, and wakes. This model was modified for atmospheric flows where stable inversion layers pass over surface undulations and areas of changing rough resistance (HUNT *et al.*, 2004). Both models showed that there are marked positive and negative perturbations in mean velocity (i.e., wind jets) that decrease gradually over transverse length scales of the order of the Rossby deformation radius L_R (30–300 km). These low-level jets, which do not occur in the absence of Coriolis effects, also exist in wake flows. These jets are associated with rising and falling airstreams which induce changes to cloudiness and precipitation. General concepts arising from these studies are reviewed in section 2.

With regard to Greenland, understanding of these jets is limited, and has mainly focused on the 'Greenland tip jet', a low-level wind jet that forms in the lee of Cape Farewell (see Fig. 1) under westerly or north-westerly synoptic conditions (DOYLE and SHAPIRO, 1999). Recently PICKART *et al.*, (2003) linked deep convection in the Irminger Sea to the southeast of Greenland with forcing by this jet. Other studies have included the wind regime over the Greenland ice sheet, and in particular katabatic flow (e.g. BROMWICH *et al.*, 1996; KLEIN and HEINEMANN, 2002), barrier jets (VAN DEN BROEKE and GALLEE, 1996), and wake flows (PETERSEN *et al.*, 2003).

Weather stations in Greenland are sparse and mostly confined to the coastal margins, predominately the southwest coast. Most of the coastal stations are run by

the Danish Meteorological Institute (DMI) and have records going back between several decades and just over a century (CAPPELEN *et al.*, 2001; JORGENSEN and LAURSEN, 2003). Within the last few years an inland network of around 20 automatic weather stations, the Greenland Climate Network (GC-Net), has been established by Konrad Steffen and colleagues (STEFFEN and BOX, 2001). Imagery collected from polar orbiting satellites can give a qualitative analyses of the surface wind patterns. For example RASMUSSEN (1989) showed that strong katabatic winds can result in a dark signature on thermal infrared satellite imagery, arising because of the turbulent mixing bringing warm upper air to the ice-covered surface, allowing the areas covered by such flows to be estimated.

Case studies for four contrasting synoptic conditions over Greenland are studied here using numerical modelling and observations. For westerly, easterly, southerly, and northerly approach winds the flows around Greenland can be approximately related to conceptual models for idealised simulations. Also they provide information which is representative of a wide number of 'in-between' synoptic conditions. The numerical model simulations combine mesoscale simulations with a horizontal resolution of approximately 12 km and ECMWF operational analysis data at $0.5^\circ \times 0.5^\circ$ resolution. The observations combine satellite imagery and the ground-based observations discussed above. The satellite pictures were obtained from a AVHRR (Advanced Very High Resolution Radiometer) onboard a polar orbiting satellite. AVHRR channel 4 (thermal infrared) was employed. Observations are included for the purpose of comparison, to corroborate model results, and to give a more comprehensive overview of meteorological conditions prevailing over southern Greenland during each of the case-study days.

The objective of this study is to further understand the influence of high orography on stable flows, and with regard to Greenland's climate processes, to improve the conceptual understanding of mesoscale meteorology of stable flows over and around Greenland: specifically the existence of low-level wind jets, their implications for atmosphere-ocean coupling, and cloudiness and precipitation. Another aspect of this work is to help improve the representation or parameterisation of mesoscale processes in numerical weather/climate prediction models (WOOD and MASON, 1993; LOTT and MILLER, 1997).

Section 2 will review low-Froude number atmospheric flows over large mountains. Section 3 will analyse the synoptic conditions for each case study. Section 4 describes the numerical mesoscale model used. Section 5 examines the flow over southern Greenland using the numerical modelling results and observations. Section 6 examines air-sea interaction. Section 7 examines cloudiness and precipitation over southern Greenland. Section 8 is a discussion.

2. Stable Flows over Large Mountains

The influence of high orography on stable flows and the local weather have long been recognised by meteorologists (e.g., BLUMEN, 1990). The significance of the additional effects of the Earth's rotation have only been recognised more recently (e.g., HUNT *et al.*, 2001; PIERREHUMBERT and WYMAN, 1985; BOYER and DAVIES, 2000). As the scales of the mountains increase to those of around continental scale plateaus, new phenomena in the characteristic wind patterns arise (see BOYER and CHEN, 1987) which are not currently parameterised or predicted by Numerical Weather Prediction (NWP) models. We focus here on north-south mountains/plateaus situated in prevailing winds, such as Greenland, the Rockies, the Southern Andes, etc. These flows are also complicated by the fact that the oncoming flow may be far from uniform in magnitude and direction over these vast scales. This causes weather systems to behave somewhat like turbulent eddies passing over or around an obstacle.

Great progress has been made in understanding and quantifying the effects of stable stratification (defined by the Brunt-Väisälä frequency N) on flow of velocity U around isolated mountains of height H, characterised by the Froude number $\mathbb{F}_H = U/NH$ which varies from ∞ to 0. This parameter characterises the strength of the inertial to buoyancy forces. For the cold, stable flows and high mountains and plateaus of interest here ($H \sim 2000 - 3000$ m; and a typical value of $N \sim 0.01$ s^{-1}), $\mathbb{F}_H$ typically lies in the range 0.2 to 0.5.

2.1. Low-Froude Number Flows without Rotation

We first consider low-Froude number flows where the effects of the Earth's rotation have a small influence on the flow near the mountain. (These effects are characterised by the Rossby number Ro ($= U/fD$, where f is the Coriolis parameter and D is the half-width of the mountain), i.e. Ro $\gg 1$). Note also the Rossby Radius of Deformation L_R ($= HN/f$). For a mountain of mesoscale dimension or smaller $B, D < L_R$ (where B is the half-length of the mountain). In this situation if $\mathbb{F}_H$ is less than about 0.5, the flow splits into the top and middle layers above and below the level z_d of the 'dividing streamline'. This lies at a distance $H_T \sim \alpha \mathbb{F}_H H$ below the top of the mountain (where $\alpha \sim 1$). z_d also varies slightly with the slope of the mountain, shear (i.e. $dU(z)/dz$) in the oncoming flow, and aspect ratio of the mountain (SNYDER *et al.*, 1985; BAINES, 1995; ÓLAFSSON and BOUGEAULT, 1996). See Fig. 2(a).

In the upper layer above z_d the streamlines pass over the mountain, but asymmetrically; ascending on the upwind side where the velocity decreases and descending on the downwind side close to the surface, where the velocity increases and internal waves are generated. In the middle layer below z_d the air flow passes in approximately horizontal planes around the mountain; as it separates on the lee side large recirculating eddies are formed. Lee waves propagate above the mountain and

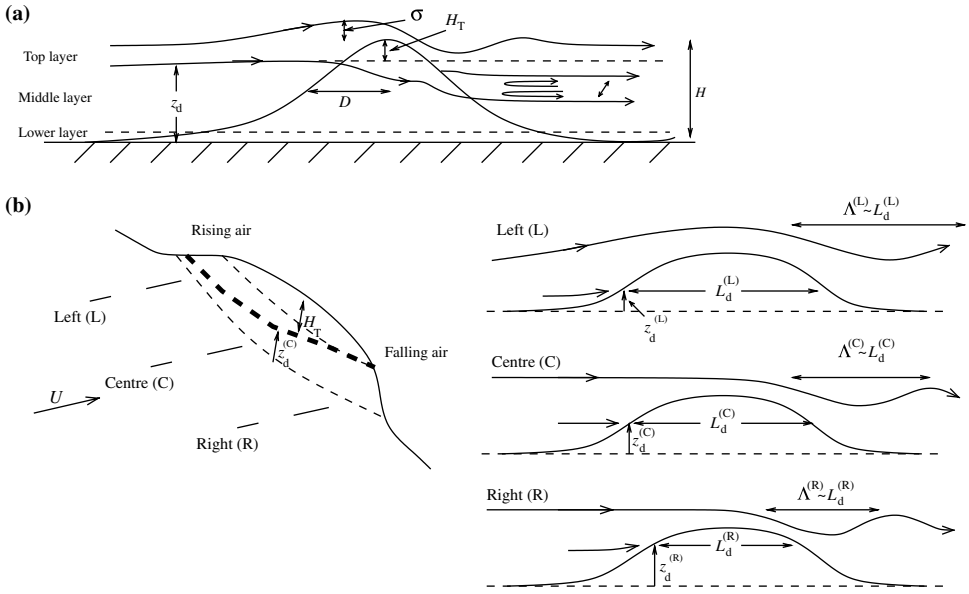

Figure 2

(a) Schematic diagram for low-Froude number flow over a mountain of mesoscale dimension with negligible Coriolis forces (i.e., Ro $\gg$ 1). D is the half-width of the mountain and H its height. z_d is the level of the 'dividing streamline'. $H_T \sim \alpha \mathbb{F}_H H$ is the distance between the dividing streamline and the mountain top. σ is the vertical streamline deflection. (b) Schematic diagram for low-Froude number flow over a long mountain with significant Coriolis forces (i.e., Ro $\sim 1 - 10$) in the northern hemisphere. Here the air flow rises on the left (looking in the downwind direction) and falls on the right. Consequently z_d is smaller and the wavelength of the lee waves, Λ, is longer on the left than the right, i.e. $z_d^{(R)} > z_d^{(C)} > z_d^{(L)}$ and $\Lambda^{(L)} > \Lambda^{(C)} > \Lambda^{(R)}$. L_d is the length of the hill (in the flow direction) at the dividing streamline height and $L_d^{(L)} > L_d^{(C)} > L_d^{(R)}$.

also down into the middle layer. In the interface between the layers intense shearing motions occur, especially on the downwind side. A third layer (the base or lower layer) is also shown. This lies beneath the middle layer and so here the air must flow around the mountain. See also Fig. 2(a).

No complete analytical model has been derived for the nonlinear flows in the upper and middle layers, though high precision numerical simulations (e.g., SMOLARKIEWICZ and ROTUNNO, 1989; DING and STREET, 2003) and an approximate model of HUNT *et al.*, (1997) have described the main features of the flows observed experimentally in the laboratory and the field (e.g. SNYDER *et al.*, 1985; VOSPER *et al.*, 1999).

2.2. Low-Froude Number Flows with Rotation

For low-Froude number flows where the effects of rotation influences the flow near the mountain (characterised by small values of the Rossby number Ro, i.e., Ro $\sim 1 - 10$), even when Coriolis forces are weak compared to the inertial or buoyancy

forces, the flow regime alters substantially and the far-field flow decays slowly on a length scale of order L_R (MERKINE, 1975; NEWLEY, *et al.*, 1991).

For a long mountain when $B \gtrsim L_R$ and $\mathbb{F}_H$ is less than about 0.5 the air flow rises on the left and sinks on the right in the northern hemisphere (looking in the downwind direction) (HUNT *et al.*, 2001). See Fig. 2(b) (based on computations of ÓLAFSSON and BOUGEAULT (1997)). This means that more low level dense air passes over the mountain, causing longer wavelength (Λ) lee waves, and a lower value of z_d, on the left than on the right. A most important feature of this left-right asymmetry and the general vertical deflection of the streamlines over the entire depth of the mountain is that greater drag is produced by the right-hand side of the mountain. Also the drag force per unit width of the mountain is of order $\rho NUH^2 \sim \rho U^2 H/\mathbb{F}_H$ (where ρ is the density of the air), which is considerably greater than the drag force of order $\rho U^2 H$ produced by the top and middle layers of a mountain when $L_R \gg B$ or $\mathrm{Ro} \gg 1$ (HUNT *et al.*, 2001; see also LOTT and MILLER, 1997).

When the Coriolis effects become even greater, so that $B/L_R \gtrsim 1/\mathbb{F}_H$, the perturbed lateral pressure gradient ($\partial p/\partial y$) associated with a large stagnant wake (e.g., $B \gtrsim 500$ km) becomes too great to be balanced by the hydrostatic pressure perturbation (Δp) associated with the vertical streamline deflection (σ), i.e., $\Delta p \sim fUB \sim \sigma N^2 H$, and since the deflection downwards cannot exceed H (i.e., $\sigma < H$), this means that $\sigma/H \sim B\mathbb{F}_H/L_R < 1$. Therefore if $B/L_R \gg 1$, to limit the vertical deflection to a physically realistic value (i.e., $\sigma < H$) the flow structure has to change so as to reduce the lateral pressure gradient (again following HUNT *et al.*, 2001).

For a mesoscale mountain or range of mountains in the northern hemisphere where $B \sim L_R$ (e.g. Pyrenees, Alps), if the approach flow is uniform this change must result firstly in flow around the left-hand side of the mountains and secondly in the large wakes or recirculation regions or synoptic eddies becoming detaching from the mountains and moving to a location downwind of the right-hand side of the mountain. This is also consistent with most of the drag being associated with the flow over the right hand part of the mountain. At the same time, because $\mathbb{F}_H < 0.5$, the approach flow streamlines still divide at height z_d between those that pass over (a 'cut-off hill') and those that pass around the mountain. A precise way to define changing flow patterns over obstacles (whether aeronautical or geophysical) is to note the location of the 'singular' points on the surface where the mean velocity is zero, and also whether they are saddle points or node points (HUNT *et al.*, 1978; HUNT and SNYDER, 1980). See Fig. 3(a).

For a synoptic scale range of mountains where $B \gg L_R$ (e.g., Greenland, Rockies) and with uniform approach flow the flow pattern changes to that shown in Fig. 3(b)(i). The saddle point S_2 that was on the downwind side of the dividing streamline in Fig. 3(a) now moves away from the mountain to the left-hand side of the detached synoptic eddies. At the same time the downwind saddle point S_3 moves to the right-hand side of the eddies. The main synoptic feature of this kind of flow is that it deflects the average flow to the right in the northern hemisphere, which leads to large

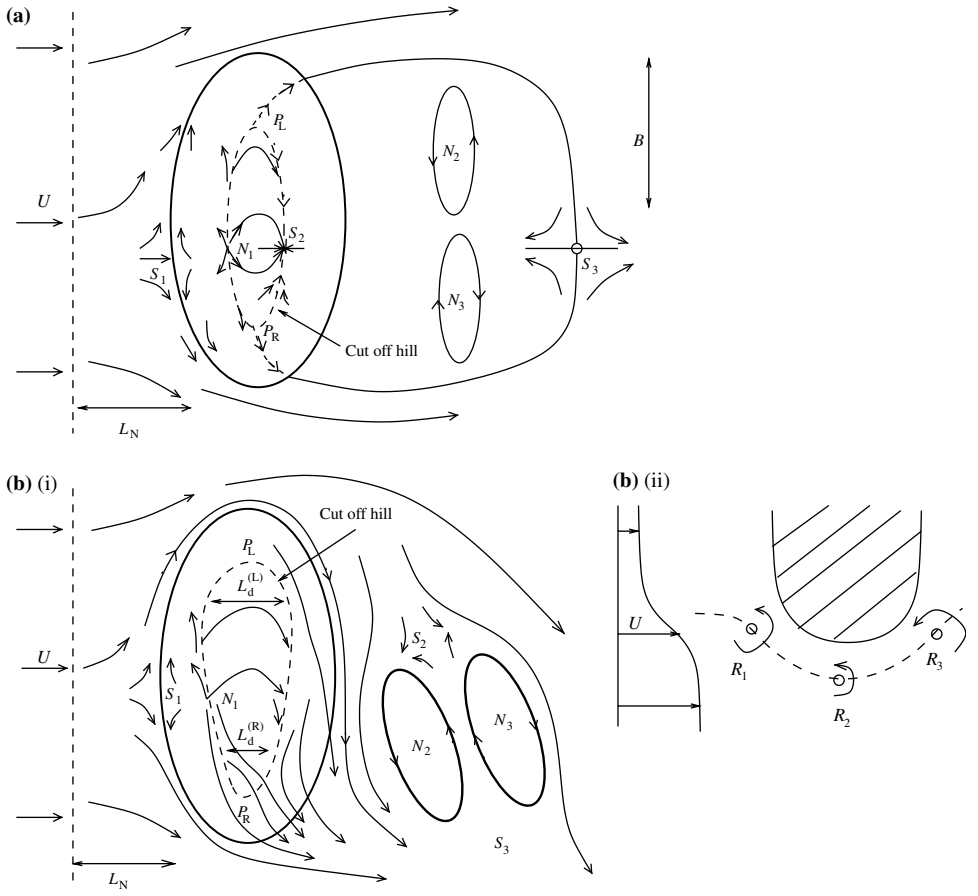

Figure 3

Near surface streamlines for low-Froude number flow in the northern hemisphere over (a) a mesoscale mountain ($B \sim L_R$) and (b) a synoptic scale mountain ($B \gg L_R$). The dividing streamline on the surface (shown as dashed line) is an attachment line upwind of P_L, P_R. S_1, S_2, S_3 are saddle points on the surface. N_1, N_2 are 'nodes'. The area defined as 'cut off hill' (shown as dashed line) is above the dividing streamline. The outline of the mountain is indicated by the thick black line. The distance L_N is the upstream deflection. In (a) the flow is greater around the left-hand side of the mountain and two recirculation regions are situated downwind of the mountain. In (b)(i) the width of the top region is greater on the left than on the right because of Coriolis effects (i.e. $L_d^{(L)} > L_d^{(R)}$). Note the separated detached pair of recirculating cyclones (eddies), which extend up to the height z_d of the dividing streamline. In (b)(ii) the local effect is sketched of northsouth shear (with cyclonic vorticity) in the approach flow.

'lift' force on the mountains to the left (HOZUMI and UEDA, 2004). This changed flow pattern was observed in laboratory experiments by BOYER and CHEN (1987) and idealised numerical simulations of ÓLAFSSON (2000).

Fig. 3(b)(ii) sketches the flow pattern if the approach flow is non-uniform. In this case southerly coastal flows are produced on the upwind side of the mountain and

northerly coastal flows on the lee side of the mountain. This can lead to concentrations of vorticity at R_1 and R_3, where the velocity decreases, but a decreased concentration of vorticity at R_2. This produces velocity *perturbations* that are in a southerly direction at R_1 and northerly at R_3, which affect the basic flows depicted in Fig. 3(a) and (b)(i).

This changed flow pattern was observed in laboratory experiments by BOYER and CHEN (1987) and idealised numerical simulations of ÓLAFSSON (2000). It is consistent with atmospheric simulations and observations of PETERSEN *et al.* (2003).

Note that if the atmosphere becomes less stable (increase in Froude number), as occurs in periods of global warming, the flow is changed quite markedly with most of the streamlines passing over the mountains, the recirculating regions becoming smaller, and the overall rightward flow deflection being greatly reduced. This may have considerable implications for the future climate to the east and southeast of Greenland and the Rocky Mountains. When the wind is directed at an acute angle to the mountain and when the approach flow is non-uniform, more complex flow patterns are expected. This is why realistic case studies are necessary.

3. Synoptic Explanation of Case Studies

Below is a short explanation of the synoptic conditions for each case study. Conditions were representative for approximately a 24-hour period. These are based on interpolation and NWP calculations, i.e., 'analysis' of UK Met Office mean sea-level pressure (MSLP). In addition, spot readings are given for representative DMI stations on the southwest coast of Greenland (04260 Paamiut and 04266 Nunarsuit), the east coast (04360 Tasiilaq), the southeastern coast (04380 Timmiarmiut and 04382 Ikermiuarsuk) and the extreme southern coast (04390 Prins Christian Sund). Data are also given for the GC-Net station South Dome (altitude 2901 m) in the southern interior. The data used are temperature at a height of 2 m and the wind velocity and direction at a height of 10 m (note for GC-Net data this height can vary depending on the amount of snow). See Fig. 1 for the locations of the stations.

3.1. Westerly Case Study (7 January, 2002)

Westerly flows are relatively rare. With prevailing easterly and northerly winds over southern Greenland, it was quite difficult to find a clear-cut westerly flow, there just being one or two cases per year.

On the 7th of January, 2002 the MSLP analysis for 00UTC (see Fig. 4(a)) shows low pressures southeast, west and east of Greenland, including in the Labrador Sea, and a weak high pressure ($\sim$992 mb) centred over the ice sheet. The infrared satellite picture for approximately 05UTC (see Fig. 4(b)) shows quite a lot of cloud in sea areas west and south of Greenland and wisps of cloud are evident over the ice sheet

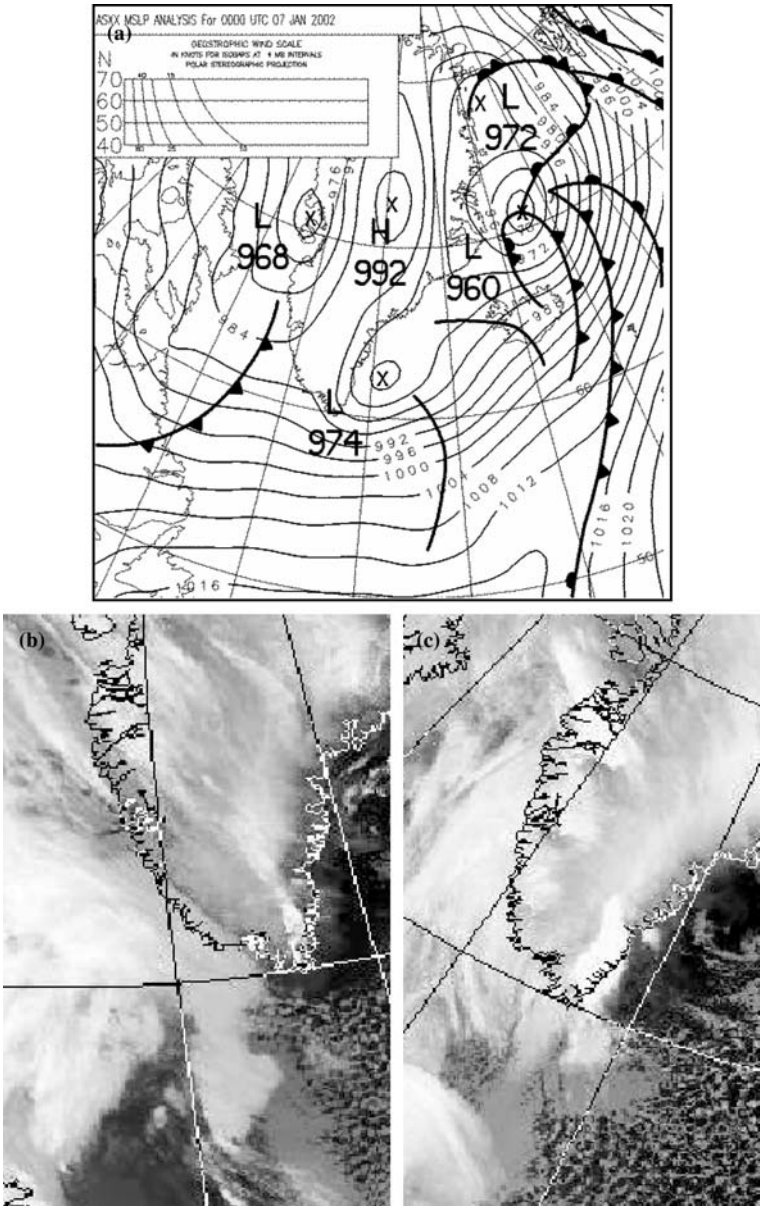

Figure 4
Synoptic analysis for 7 January, 2002 (westerly case). (a) UK Met Office MSLP analysis for 00UTC. (b) Infrared satellite image at 05UTC. (c) Infrared satellite image at 15UTC.

itself (only partly clear conditions). During the course of the day the cloud travelled across southern Greenland (see Fig. 4(c)). Table 1 shows the station reports for 00UTC indicating a westerly flow incident to the southern tip of Greenland.

Table 1

Station reports for 00UTC 7 January, 2002 (westerly case)

Station	Temperature (°C)	Wind speed (ms^{-1})	Wind direction (°)
04260	−3.4	4.1	280
04360	−3.3	1.5	260
04390	−1.1	8.2	230
South Dome	−28	3.1	299

Conditions were relatively 'mild' for winter under this westerly flow regime. During the course of the day the synoptic airflow changed to more south-westerly as a low developed over the Labrador Sea. Meanwhile, the surface high intensified over the ice sheet, displacing the complex lows to the east and southeast.

3.2. Easterly Case Study (26 January, 2002)

Easterly flows are common in Greenland, especially in the north-west where they predominate ~24–38% of the time (CAPPELEN *et al.*, 2001). They are typically marked by high pressure over northern Greenland.

On the 26th of January, 2002 the MSLP analysis for 00UTC (see Fig. 5(a)) shows a large, deep (964 mb), but not particularly intense, low pressure lying ~500 km south of Greenland, with relatively high pressure over the Canadian Arctic and

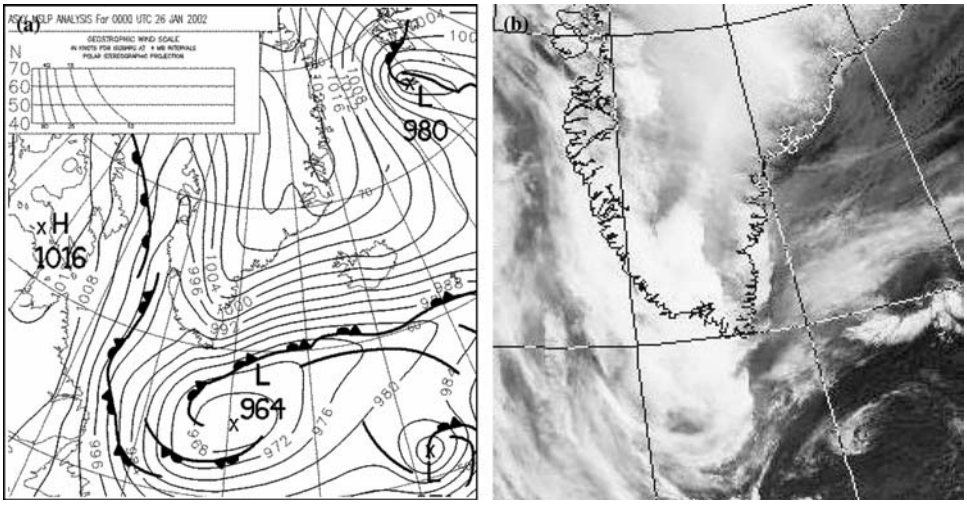

Figure 5
Synoptic analysis for 26 January, 2002 (easterly case). (a) UK Met Office MSLP analysis for 00UTC. (b) Infrared satellite image at 05UTC.

Table 2

Station reports for 12UTC 26 January, 2002 (easterly case)

Station	Temperature (°C)	Wind speed (ms^{-1})	Wind direction (°)
04260	−8.4	0.5	30
04266	1.2	6.7	60
04360	−12.2	1.0	30
04382	−3.7	22.1	340
04390	−1.9	24.7	20
South Dome	−31	8.8	69

northern Greenland. The depression was fully mature, as marked by its three occluded fronts and broken spiral cloud bands (see Fig. 5(b)), and beginning to fill and decay (969 mb by midnight). The depression was a near-stationary feature throughout the day. Iceland, the Denmark Strait and southern Greenland were engulfed in a strong persistent east/north-easterly flow, causing the development of a foehn trough over southwest Greenland. The infrared satellite picture for approximately 05UTC (see Fig. 5(b)) shows wisps of cloud streaming westwards along the main front across the Norwegian Sea and into southernmost Greenland. However, the bulk of Greenland was under clear skies. Table 2 shows the station reports for 12UTC. Conditions were cold—very cold at South Dome. Most of the station reports show a strong northeast wind incident on Southern Greenland.

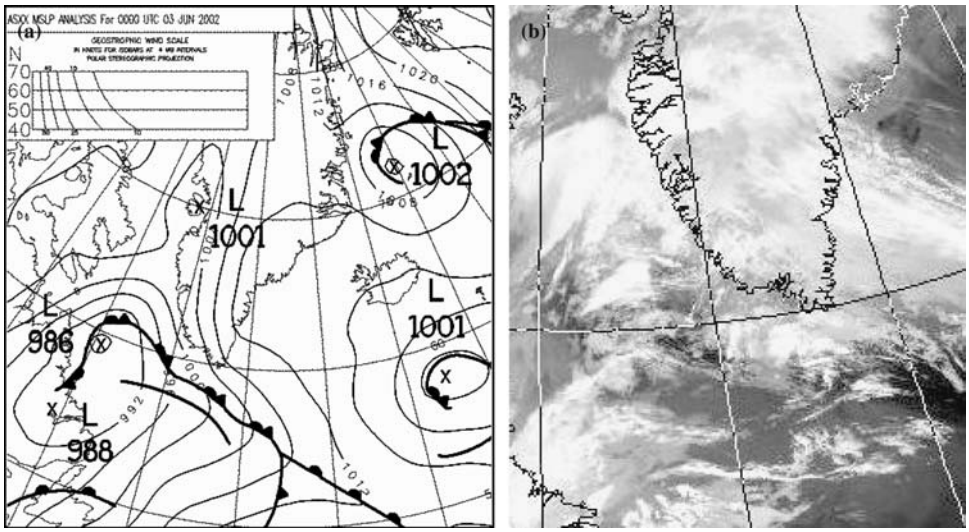

Figure 6
Synoptic analysis for 3 June, 2002 (southerly case). (a) UK Met Office MSLP analysis for 00UTC. (b) Infrared satellite image at 05UTC.

3.3. Southerly Case Study (3 June, 2002)

Southerly flows are by implication mild and moist, emerging as they do from a relatively warmer ocean. Distinct cases are relatively uncommon and they typically occur with a low-pressure system anchored southwest of Greenland and tend to yield precipitation around the southern and south-south-west margins.

On the 3rd of June, 2002 the MSLP analysis for 00UTC (see Fig. 6(a)) shows a complex shallow area of low pressure lying anchored off southwest Greenland, with its occluded frontal system just clipping the southern tip. This fed a relatively mild south-south-easterly airflow over southern Greenland. (This case is unique in being near midsummer; the others are all winter cases.) The infrared satellite picture for approximately 05UTC (see Fig. 6(b)) shows patchy clouds over the southern half of Greenland. There were further low pressure systems situated on the west coast of Greenland and south of Iceland. Table 3 shows the station reports for 12UTC. A couple of the stations (04266 and 04360) have a near southerly wind; the others have something closer to a northerly! Perhaps this resulted from local effects (e.g., sea breeze at 04360) and the relatively slack pressure gradient away from the southernmost tip of Greenland.

3.4. Northerly Case Study (21 February, 2002)

Northerly flows with cold polar air plunging south over Greenland are very typical due to frequent formation and deepening of low pressure systems between Greenland and Iceland. According to a table of 1961–1990 climatological standard normals in CAPPELEN *et al.*, (2001), north is the most frequent wind direction at the capital of Greenland Nuuk on the southwestern coast (21% of cases), and on the northeastern coast and in the extreme southeast (e.g., Prins Christian Sund, 28% of cases). HANNA and CAPPELEN (2003) demonstrated that temperature over southern (particularly southwest coastal) Greenland in the past few decades is strongly

Table 3

Station reports for 12UTC 3 June, 2002 (southerly case)

Station	Temperature (°C)	Wind speed (ms^{-1})	Wind direction (°)
04260	4.9	2.1	320
04266	3.2	14.9	190
04360	2.8	1.0	200
04382	2.6	7.7	330
04390	3.1	9.8	10
South Dome	−11	8.9	138

associated with changes in the North Atlantic Oscillation (NAO), and as the NAO became more positive, overall temperature declined between 1958 and 2001. This is linked in all likelihood with a greater frequency/persistence of strong, cold northerly winds over Greenland.

On the 21st of February, 2002 the MSLP analysis for 00UTC (see Fig. 7(a)) shows a complex and deepening area of low pressure centred in the Denmark Strait (between Greenland and Iceland), with increasingly higher pressure westwards over the Labrador Sea. There was an eastwest pressure gradient of ~40 mb across the Denmark Strait/southern Greenland at 00UTC, which was maintained and even strengthened during the next 24 hours, increasing to ~70 mb by 00UTC on 22 February (not shown). Consequently Greenland was in the grip of a strong northerly air stream. The infrared satellite picture for approximately 15UTC (see Fig. 7(b)) shows a very well-defined frontal cloud band aligned southwest to northeast, over the Atlantic lying well to the south of Greenland, with the centre of the low apparent just west of Iceland. An intricate herringbone structure of partly open cloud cells suggests strong convection in destabilised polar air as it hit open waters around the south of Greenland. The entire Greenland ice sheet appears white and extremely cold in clear skies, leading to large radiative heat loss (~-22 Wm^{-2} at South Dome at 12UTC and -49 Wm^{-2} at 15UTC). The area immediately around Iceland, including the Denmark Strait, was considerably cloudier with very large convective cloud cells. Table 4 illustrates the extremely cold conditions at 12UTC.

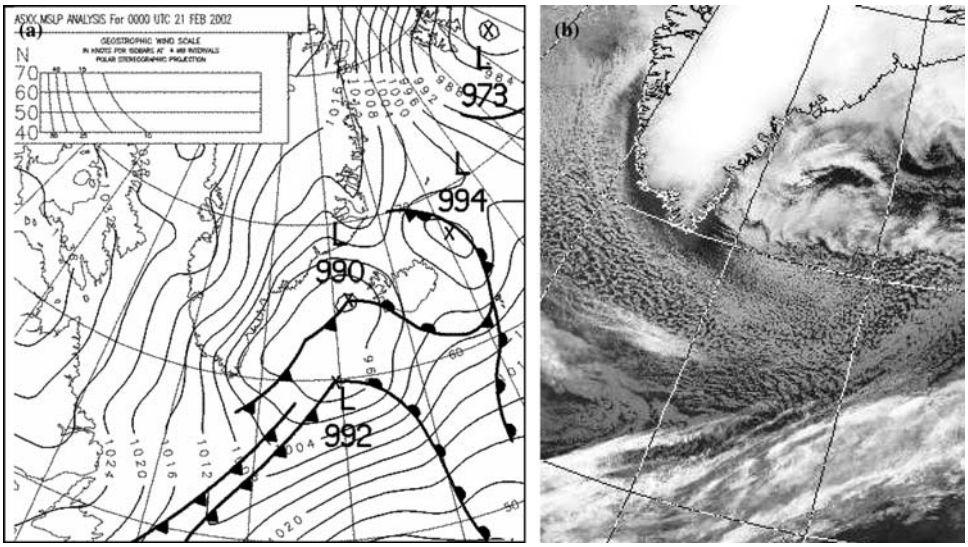

Figure 7
Synoptic analysis for 21 February, 2002 (northerly case). (a) UK Met Office MSLP analysis for 00UTC. (b) Infrared satellite image at 15UTC.

Table 4

Station reports for 12UTC on 21 February, 2002 (northerly case)

Station	Temperature (°C)	Wind speed (ms^{-1})	Wind direction (°)
04260	−18.6	5.1	350
04266	−11.4	20.6	320
04360	−16.7	4.1	330
04382	−15.2	11.3	320
04390	−9.5	13.4	270
South Dome	−51	15.2	322

It also shows a north or north-westerly wind travelling parallel to the east and west coasts of Greenland.

4. Numerical Mesoscale Model

The numerical model used is the atmosphere-only UK Met Office Unified Model (UM). The UM is a General Circulation Model (GCM) designed to run either as a climate model or a NWP model. As a climate model it was shown to generally simulate realistically the Antarctic climate, in particular the strong surface winds which are similar to those of Greenland (CONNOLLEY and CATTLE, 1994). Here the model is run in NWP mode as a mesoscale model. Version 4.5 is implemented (UM 4.5).

UM 4.5 employs a non-linear, hydrostatic set of dynamical equations on a horizontal latitude-longitude grid. A Lorenz grid is used in the vertical with a 'hybrid' sigma/pressure coordinate system giving increased resolution near the ground and the troposphere. CULLEN (1993) provides a description of the numerical formulation of the model. The physical parameterisations include schemes to represent boundary layer mixing, convection, precipitation, surface exchange, cloud formation, and shortwave and longwave radiation (CLARK and HOPWOOD, 2001). UK Met Office operational analyses data are used to initialise the model.

A limited-area domain was used with uniform resolution within the domain achieved through a rotated pole, i.e., the coordinate pole is not placed at the centre of the domain. Lateral boundary conditions are generated by nesting the limited-area domain within UM 4.5 running as a global model (CULLEN, 1993). The domain size was a 182 by 146 latitude-longitude grid with 0.11° ($\sim$ 12 km) resolution and 38 model levels in the vertical. (The domain configuration for the global model is a 325 by 432 latitude-longitude grid with resolution 0.83° by 0.56° and 30 model levels in the vertical.)

5. Flow over Greenland

In this section we analyse the flow over Greenland for each of the case studies using the combination of modelling and observational data. Note that over southern Greenland the Rossby deformation radius is approximately 230 km (for $f \sim 1.3 \times 10^{-4}$ s^{-1}, $H \sim 3000$ m, and $N \sim 0.01$ s^{-1}).

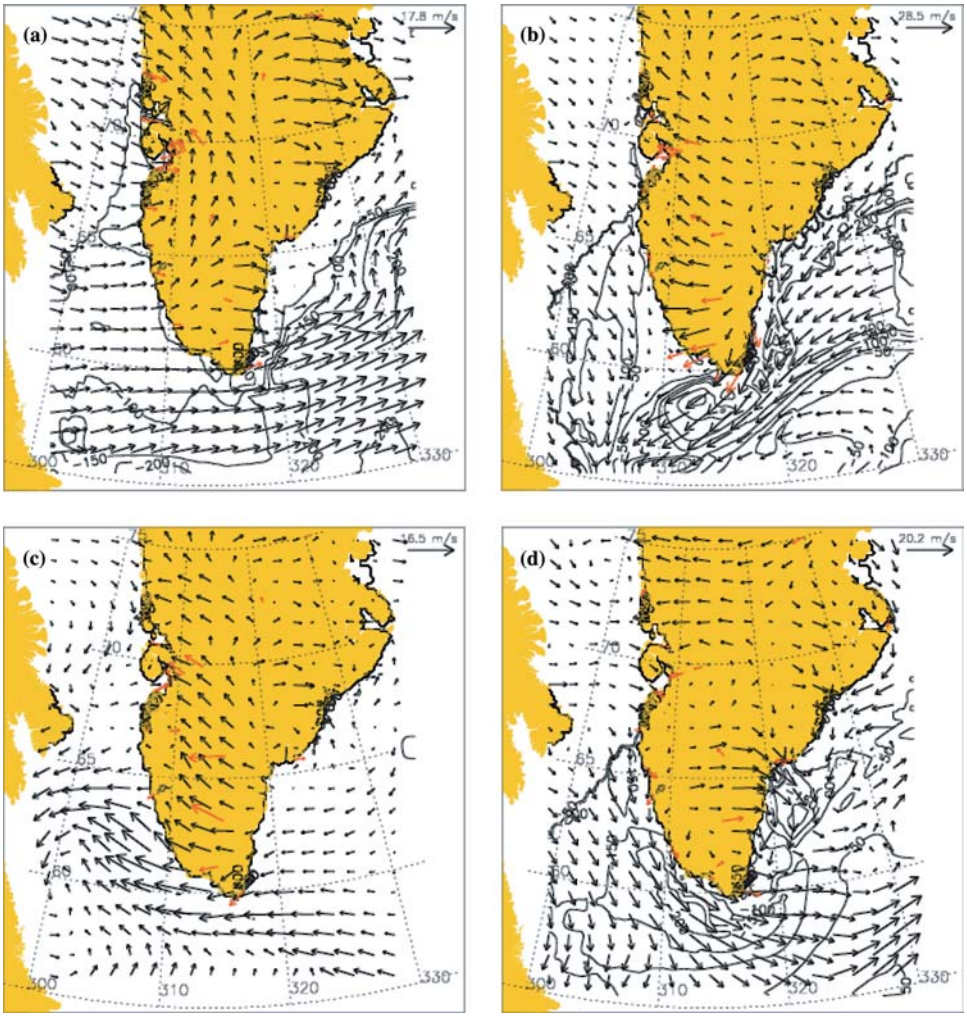

Figure 8
Variation of 10-m wind speed (shown as wind vectors (ms^{-1})) and latent heat flux (shown as contours (Wm^{-2})) over Southern Greenland at (a) 01UTC 7 January, 2002 (westerly case), (b) 06UTC 26 January, 2002 (easterly case), (c) 01UTC 3 June, 2002 (southerly case), and (d) 00UTC 21 February, 2002 (northerly case). Computed using UM 4.5 at a horizontal resolution of 12 km. (Wind speed vectors are averaged over 8 grid points.) DMI and GC-Net observations are shown in red.

5.1. Westerly Approach Flow

Figure 8(a) shows UM 4.5 simulated 10-m wind speeds at 01UTC 7 January, 2002 of a westerly flow of approximately 5–7 ms^{-1} incident to Greenland (giving $\mathbb{F}_H \approx 0.2$) (to the northwest the flow is slightly northerly). Because of the steep coastal terrain the flow slows as it travels into Greenland. Consequently it is deflected to the left due to Coriolis where it combines with the katabatic winds which, due to

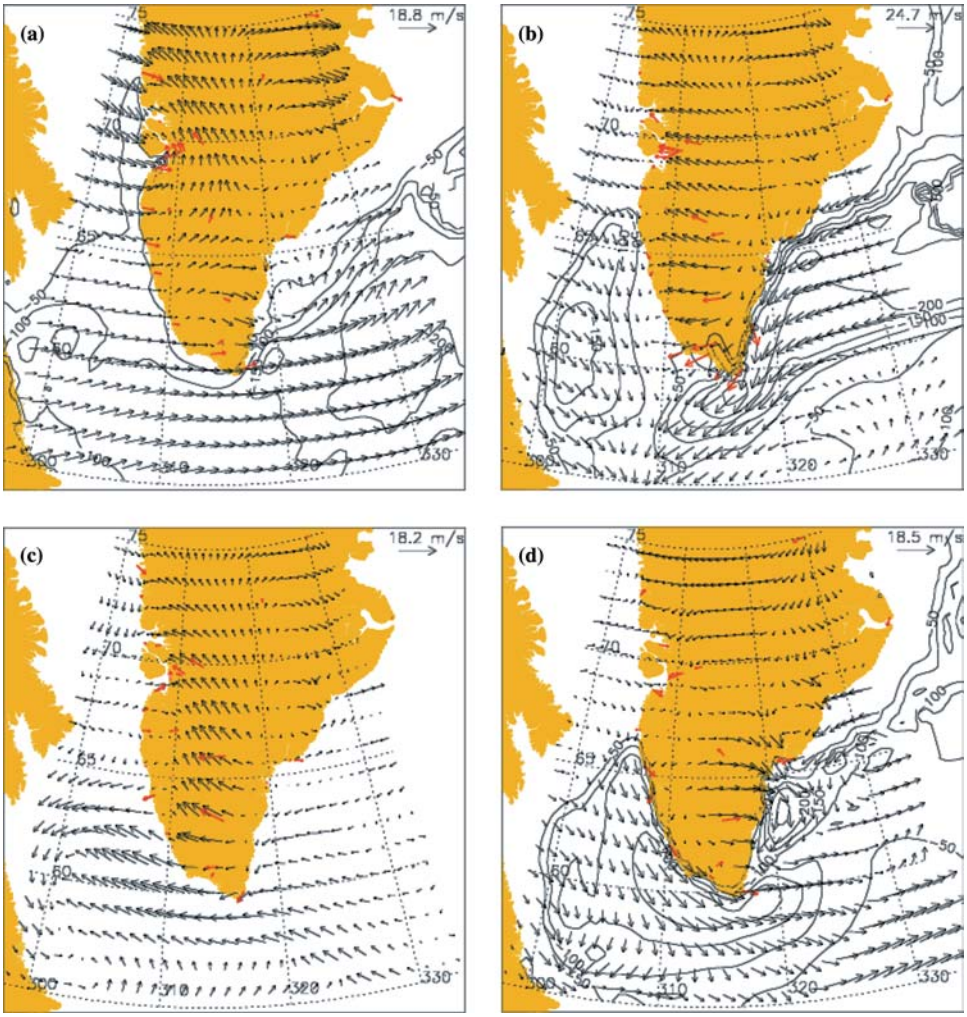

Figure 9
Variation of 10-m wind speed (shown as wind vectors (ms^{-1})) and latent heat flux (shown as contours (Wm^{-2})) over southern Greenland at (a) 00UTC 7 January, 2002 (westerly case), (b) 06UTC 26 January, 2002 (easterly case), (c) 00UTC 3 June, 2002 (southerly case), and (d) 00UTC 21 February, 2002 (northerly case). From ECMWF operational analysis data. DMI and GC-Net observations are shown in red. (The latent heat flux data are averaged over a three-hour period from the times shown.)

the slope of the ice sheet (see Fig. 1), are predominately south-easterly. This is confirmed by the DMI observations shown in red in Fig. 8(a) and 10-m wind ECMWF operational analysis data for 00UTC (see Fig. 9(a)).

At the 700 mb height (which is roughly the same height as the summit of Greenland) the UM 4.5 simulated winds show a strengthening in the upstream velocity, and to the northwest of Greenland the flow is much reduced and

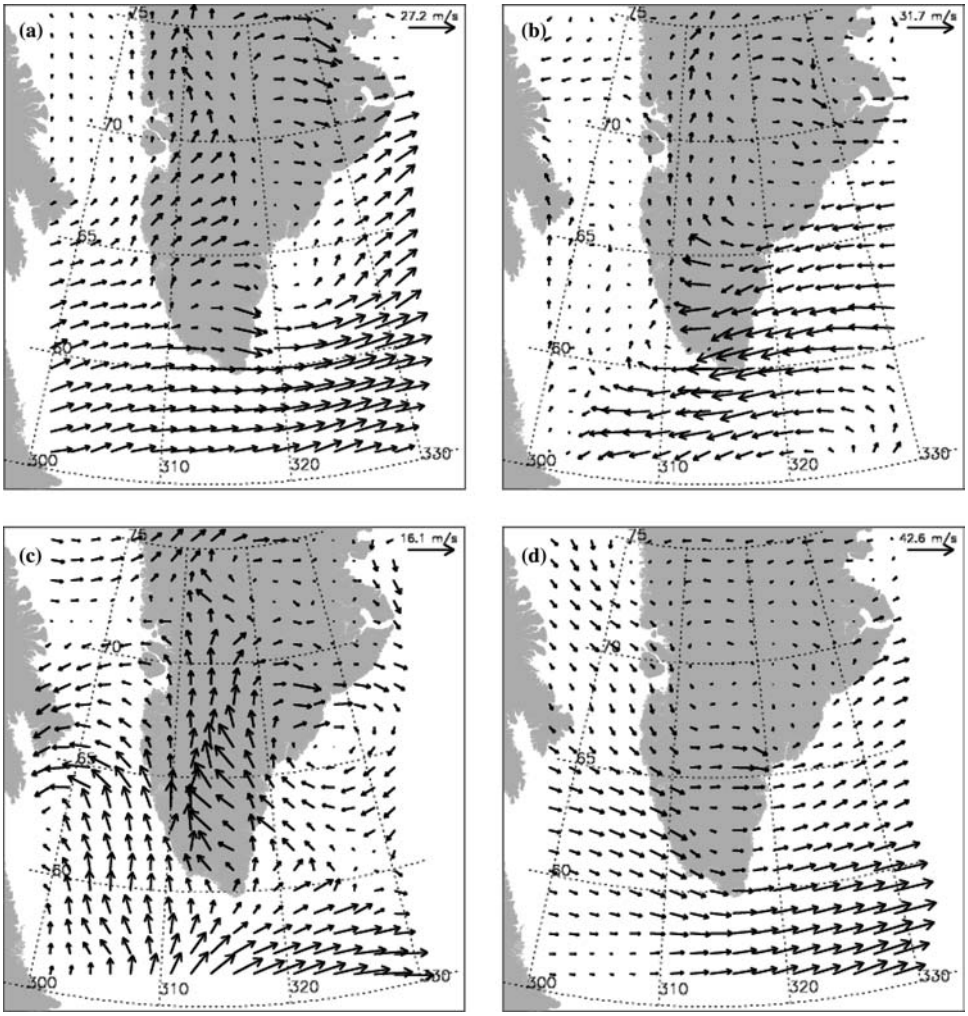

Figure 10
Variation of 700 mb wind speed (shown as wind vectors (ms^{-1})) over southern Greenland at (a) 01UTC 7 January, 2002 (westerly case), (b) 06UTC 26 January, 2002 (easterly case), (c) 01UTC 3 June, 2002 (southerly case), and (d) 00UTC 21 February, 2002 (northerly case). Computed using UM 4.5 at a horizontal resolution of 12 km. (Wind speed vectors are averaged over 8 grid points.)

predominately southerly (see Fig. 10(a)). At this level as the flow travels into Greenland it is only partially slowed and deflected. However, 700 mb flow does not pass over the summit. Rather it is blocked and rapidly deflected to the left where it merges with the katabatic winds over the plateau (c.f. Fig. 3(b)(i)). (Over the plateau the GC-Net observations show good agreement with the UM 4.5 700 mb wind field (not shown).) At 500 mb height (see Fig. 11(a)) the flow passes over Greenland with little deflection (though at this height the upstream winds are predominately

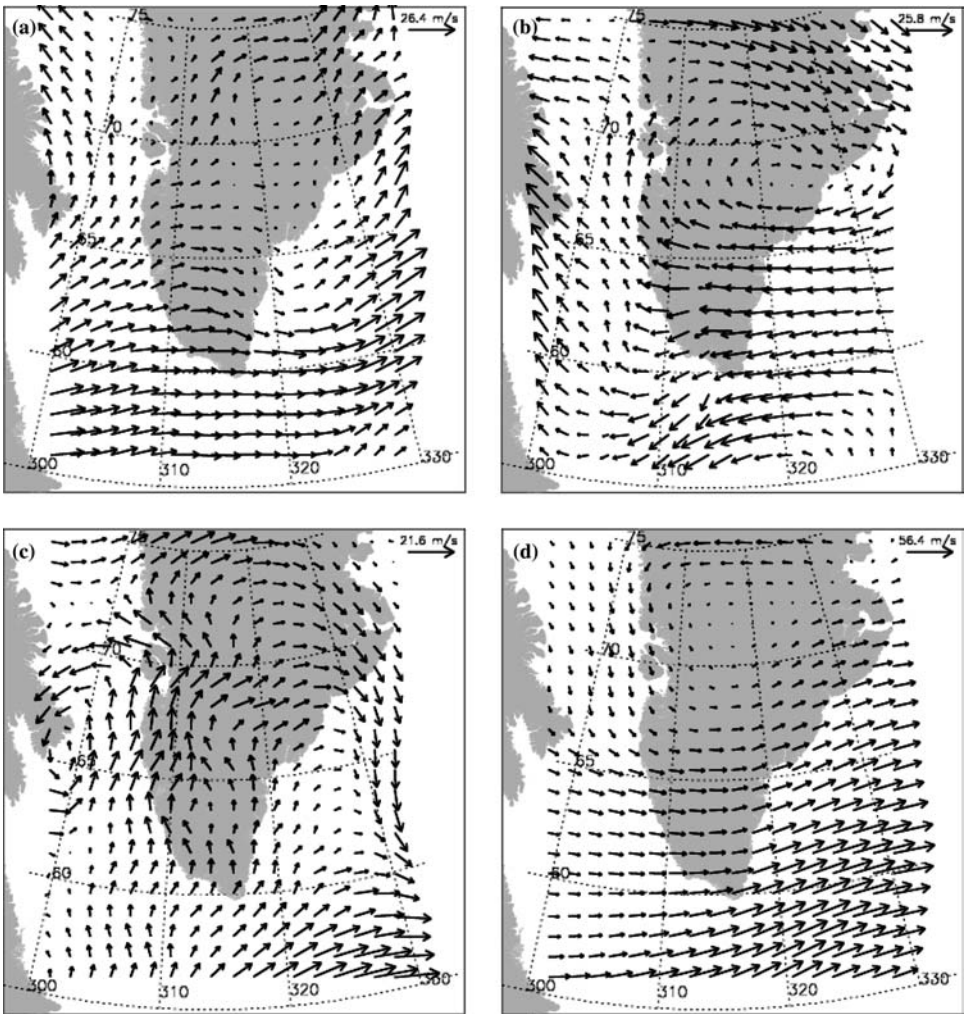

Figure 11
Variation of 500 mb wind speed (shown as wind vectors (ms^{-1})) over Southern Greenland at (a) 01UTC 7 January, 2002 (westerly case), (b) 06UTC 26 January, 2002 (easterly case), (c) 01UTC 3 June, 2002 (southerly case), and (d) 00UTC 21 February, 2002 (northerly case). Computed using UM 4.5 at a horizontal resolution of 12 km. (Wind speed vectors are averaged over 8 grid points.)

southerly due to the low pressure system sitting to the west of Greenland (see Fig. 4(a)).

Over southern Greenland the 10-m wind is well defined upstream and approximately 7–9 ms^{-1} (see Fig. 8(a)). The simulations and observations show the flow passing around the extreme southern tip of Greenland. As the flow to the south of the Greenland approaches the tip it accelerates to around 9–13 ms^{-1}, forming a jet. It continues to accelerate and be deflected to the left as it passes the tip. At station 04390, observations show the wind speed as approximately 8 ms^{-1} and south-westerly (see Table 1 and Fig. 8(a)). The width of the jet here is greater than 500 km (i.e. $> L_R$). The flow reaches its maximum velocity of approximately 17 ms^{-1} in the wake, an increase of over 100%, around 300 km downwind of Cape Farewell. In this wake region the wind vectors in surface (and 700 mb) plots appear to (re)curve slightly to the right up to several hundred kilometres downstream of Cape Farewell (not purely synoptic factors). In the wake the flow gradually slows and becomes more southerly due to the low pressure to the east of Greenland (see Fig. 4(a)). The 10-m wind ECMWF data for 00UTC show the flow being deflected as it passes the tip, though it gives a marginally stronger speed up in the wake of around 18 ms^{-1}. Note that in other synoptic situations over southern Greenland with a more uniform approach flow (e.g., HUNT *et al.*, 2004 – 9 November, 2000), westerly flows lead to southerly winds in the wake of the easterly side of Greenland (as in the idealised and numerical results of Fig. 3(b)(i)).

At the 700 mb height the UM 4.5 simulation shows stronger westerly winds across southern of Greenland. The upstream velocity is approximately 15 ms^{-1}, which accelerates to around 20 ms^{-1} just south of the tip, and eventually reaching around 25 ms^{-1} in the wake. At 500 mb the flow speed across southern Greenland is considerably more uniform, roughly 17–20 ms^{-1}. For both 500 mb and 700 mb winds the flow in the wake of Greenland is deflected to the north.

Over the plateau itself the UM 4.5 and ECMWF data both indicate that near the surface katabatic winds dominate. South-easterly katabatic winds are evident in the western part of Greenland. While on the eastern side of Greenland the winds are predominately westerly reflecting the slope in that region. Both sets of data show the wind speed increasing towards the coastal margins of Greenland and significant interaction with the synoptic flow. This flow pattern is still largely evident at 700 mb, as discussed above. However, winds at 500 mb height are largely dominated by the synoptic flow.

5.2. Easterly Approach Flow

Fig. 8(b) shows UM 4.5 simulated 10-m wind speeds at 06UTC 26 January, 2002 of an upstream region characterized by a relatively strong, low-level east/north-easterly flow of about 13–15 ms^{-1} (giving $\mathbb{F}_H \approx 0.45$). This is blocked by the very steep mountains of the east coast of Greenland, forcing the flow south and parallel to

the coast. The flow parallel to the coastline accelerates as it travels south and curves left, forming a barrier jet, and increasing from approximately 8 to 25 ms^{-1} between 70°N and the southern tip, an increase of over 200% (also shown by ECMWF operational analysis in Fig. 9(b)). Observational data show the wind speed at 10 m height at the southeastern coast as approximately 22 ms^{-1} at station 04382 and as approximately 25 ms^{-1} at station 04390 (see Table 2). The width of the jet here is roughly 300–500 km (i.e., of the same order as L_R). Additional UM 4.5 contoured data (not shown) showed very sharp gradients in the velocity perpendicular to the coastline. The velocity of the flow decreases gradually in the wake downstream of Cape Farewell. In this wake region the wind vectors curve slightly to the right due to the deep, low pressure system situated south of Greenland (see Fig. 5(a)). Fig. 8(b) shows easterly katabatic winds from the ice sheet interacting with the synoptic winds at the coastline, increasing these gradients. As the jet passes the tip it curves slightly to the right (looking downwind) and its velocity begins to decrease. Additional contour data show very sharp velocity gradients at the edges of the jet.

At the 700 mb height the upstream region is well defined as a easterly flow with a velocity of around 11–15 ms^{-1}. The flow travels over southern Greenland and is gradually blocked and deflects to the left (looking downwind). An infrared satellite image (see Fig. 5(b)) confirms this as it indicates mid-level frontal cloud being blocked slightly inland of the southeastern coast (c.f. Fig. 3(b)(i)). Over the western side the 700 mb flow is shown accelerating and being deflected to the right. The GC-Net observations over the plateau show good agreement with the flow at this height (not shown). Over the extreme tip of Greenland the flow accelerates, increasing to around 25 ms^{-1}, or around twice the upstream velocity, suggesting that the jet's vertical scale is of the order of ~ 1000 m. A synoptic high is stationed over the main plateau.

The simulated 500 mb flow (see Fig. 11(b)) shows much less deflection due to Greenland itself and a greater emphasis on (mid-tropospheric) synoptic wind fields.

5.3. Southerly Approach Flow

Fig. 8(c) shows UM 4.5 simulated 10-m wind speeds at 01UTC 3 June, 2002 of an upstream region characterised by a low-level southerly flow of 5–7 ms^{-1} (giving $\mathbb{F}_H \approx 0.2$). Part of the upstream flow is south-easterly which deflects the southerly flow to the left and increases its velocity as it approaches Greenland. As the flow travels north parallel to the western coastline its velocity accelerates from around 9 ms^{-1} to 15 ms^{-1} between the tip of Greenland and around 63°N, or by about 80%. The width of the jet here is roughly 300–500 km. Observational data show the wind speed at 10 m height as approximately 15 ms^{-1} at station 04266 (at 12UTC; see Table 3). And also it is deflected to the left due to Coriolis. To the north of 63°N the flow is deflected further to the left by the low pressure system situated off the west coast of Greenland (see Fig. 6(a)). Fig. 8(c) shows

predominately south-easterly katabatic winds interacting with the synoptic winds along the western coastal margin. This is confirmed by the DMI observations shown in red in Fig. 8(c) and 10-m wind and ECMWF operational analysis data for 00UTC (see Fig. 9(c)).

The single observation (04390) near the tip of Greenland at 12UTC shows a velocity of around 10 ms^{-1} and in an almost northerly direction. This is also evident 12 hours earlier in the UM 4.5 and ECMWF 10-m wind data (though more easterly). This could represent part of a katabatic (shallow-layer) flow off the ice cap. No equivalent northerly wind vectors are seen in the 700 and 500 mb height data (see Fig. 10(c) and 11(c)), suggesting that the postulated low-level katabatic flow is indeed shallow. The higher level plots also indicate a considerably more linear south-to-north flow over Greenland. The 700 mb plot has flow accelerating quite markedly northwards over southern Greenland as it breaks over the southern ice dome (South Dome in Fig. 1). No such acceleration is evident in the 500 mb plot and this suggests that flow is undisturbed at this level. At both levels the flow to the west and east of Greenland is strongly deflected due to the low pressure systems sitting to the west and east of Greenland (see Fig. 6(a)).

5.4. Northerly Approach Flow

Fig. 8(d) shows UM 4.5 simulated 10-m wind speeds at 00UTC 21 February, 2002 of an upstream region characterised by a relatively weak, low-level westerly flow of $\sim$ 5 ms^{-1} (giving $\mathbb{F}_H \approx 0.1$) between 67°N and 75°N. This is blocked by the mountains of the west coast of Greenland, forcing the flow south. This northerly flow develops into a distinct barrier jet travelling parallel to the coastline and increasing in velocity with distance propagated. Inspection of contoured data show sharp gradients of velocity parallel to the coastline. Between 67°N and the tip of southern Greenland its wind speed increases from about 5 ms^{-1} to 17 ms^{-1}, or by about 240%. Observational data show the wind speed at 10 m height as approximately 5 ms^{-1} at station 04260 and as approximately 21 ms^{-1} at station 04266 (at 12UTC; see Table 4). The width of the jet here is approximately 500 km. As the jet passes around the tip it curves markedly to the left (looking downwind), due to the combination of Coriolis and interaction with the low pressure system centred in the Denmark Strait (see Fig. 7(a)). The wind jet continues as a westerly flow downwind of the tip in its wake, its velocity decreasing gradually. The UM 4.5 10-m wind speeds also show a slight deflection of the low-level flow to the right in the wake of the southern mountains of Greenland (within the region several hundred kilometres southeast of Cape Farewell). This is confirmed by the DMI observations shown in red in Fig. 8(d) and 10-m wind ECMWF operational analysis data for 00UTC (see Fig. 9(d)).

Fig. 8(d) shows strong westerly katabatic winds over southern Greenland being funnelled down to the ocean (perhaps through the Angmagssalik fjord (RASMUSSEN, 1989)) and interacting with the cyclonic flow to the east of Greenland.

Upper air flows at 700 and 500 mb height (see Figs. 10(d) and 11(d), respectively) also show northerly flow west of Greenland, curving westerly and increasing markedly in strength further south around Cape Farewell. However this speed-up could not be termed a jet as it applies to a very large band of the flow (> 1000 km wide) and is linked with the low pressure system centred in the Denmark Strait.

6. Air-sea Interaction around Greenland

Here a negative heat flux is defined as the direction from the surface to the atmosphere (i.e., cooling of the surface).

6.1. Westerly Approach Flow

The strong speed-up jet evident southeast of Greenland and discussed in section 5.1 is commonly called the Greenland tip jet. It is associated with cold temperatures (see Table 1) and corresponds here to regions of large negative surface heat flux. Figs. 8(a) and 9(a) show UM 4.5 and ECMWF modelled latent heat fluxes of up to -200 Wm^{-2} (i.e., strong cooling of the surface due to evaporation). Figs. 12(a) and 13(a) show a slightly smaller sensible heat flux of around -100 to -150 Wm^{-2} in the speed-up jet region. This suggests that for this case study evaporation associated with the jet, more than the jet itself, is cooling the sea-surface southeast of southern Greenland. As the surface water cools it becomes more dense and sinks, resulting in downwelling (PICKART *et al.*, 2003). Additionally, Figs. 8(a) and 9(a) show the jet curving sharply to the left, resulting in a strong, localised wind stress curl. Due to Ekman motion this would create a cyclonic or divergent gyre in the ocean, which will also result in downwelling (GILL, 1982; PICKART *et al.*, 2003).

6.2. Easterly Approach Flow

There are large, negative heat fluxes of up to -200 Wm^{-2} (both sensible and latent) in the Denmark Strait, stretching and narrowing into a region corresponding to the speed-up jet discussed in Section 5.2, which extends southwest of Cape Farewell on the southern tip. The jet here is both colder (see Table 2) and stronger than the previous westerly case, explaining perhaps why both the modelled sensible heat fluxes (see Figs. 12(b) and 13(b)) and latent heat fluxes (see Figs. 8(b) and 9(b)) are slightly larger. We therefore have cooling and evaporation of relatively warm sea water, resulting in downwelling. From Figs. 8(b) and 9(b) there is only a slight curving of the wind vectors and therefore weak wind stress curl. Upstream of Cape Farewell weak downwelling might occur. But downstream of Cape Farewell the

rightward turning wind vectors would produce a weak convergent gyre and weak upwelling (GILL, 1982).

6.3. Southerly Approach Flow

There are small, positive sensible heat fluxes of about 50 Wm^{-2} in a narrow region just south and southwest of Greenland, corresponding to the barrier jet travelling north and parallel to the western coastline and discussed in Section 5.3

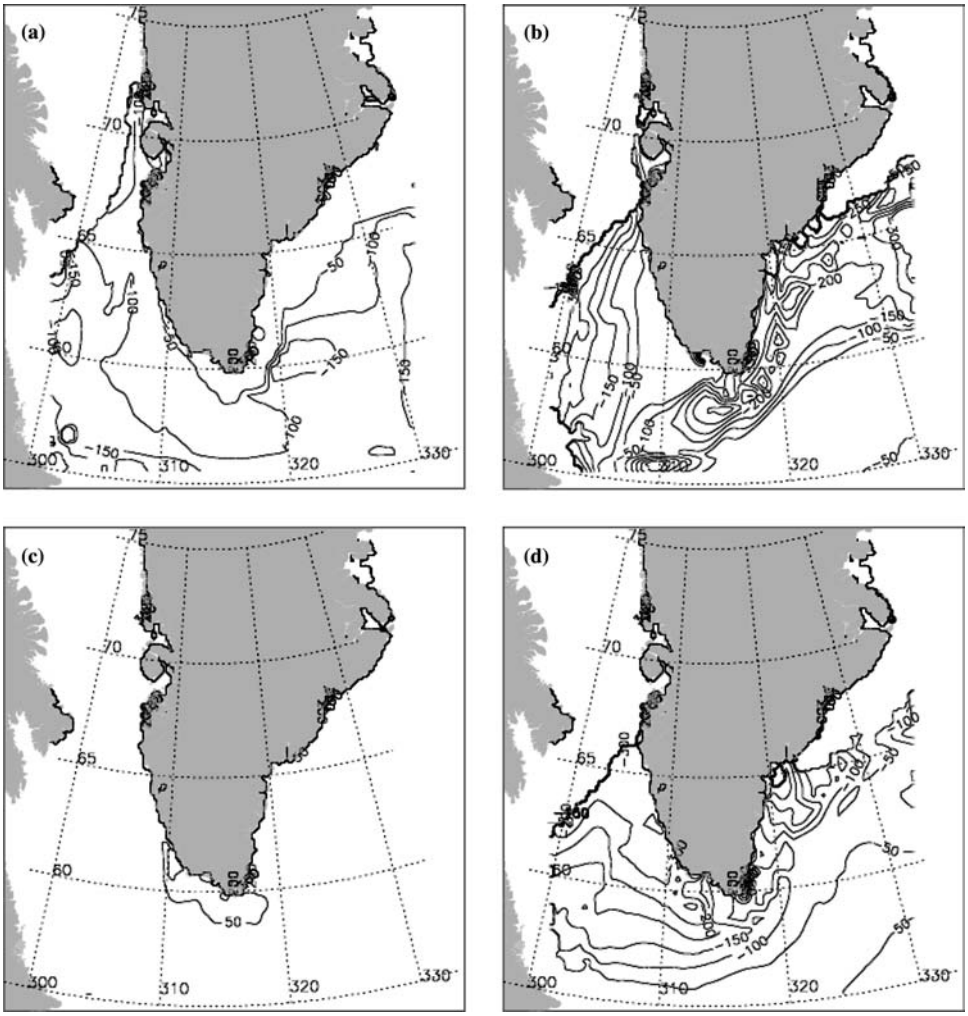

Figure 12
Variations of sensible heat flux (Wm^{-2}) over southern Greenland at (a) 01UTC 7 January, 2002 (westerly case), (b) 06UTC 26 January, 2002 (easterly case), (c) 01UTC 3 June, 2002 (southerly case), and (d) 00UTC 21 February, 2002 (northerly case). Computed using UM 4.5 and a horizontal resolution of 12 km.

(see Figs. 12(c) and 13(c)). There are no significant areas of latent heat fluxes (see Figs. 8(c) and 9(c)). This is because this southerly, near-midsummer flow (air of temperate or even subtropical origin; see Table 3) would not be expected to cool the sea surface or cause evaporation, but it would itself perhaps been modified (cooled) somewhat by passage over the relatively cool ocean (therefore would probably not cause a very substantial warming either). Figs. 8(c) and 9(c) show

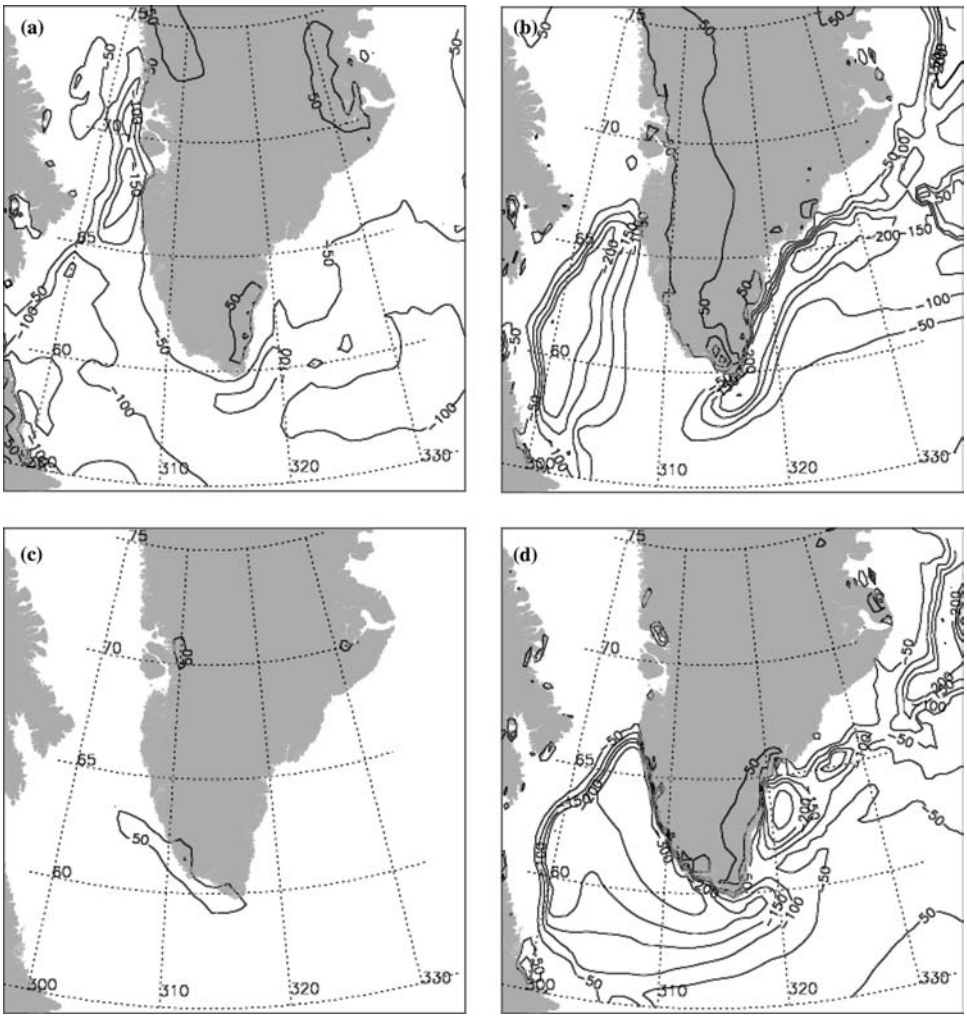

Figure 13
Variations of sensible heat flux (Wm^{-2}) over southern Greenland at (a) 00UTC 7 January, 2002 (westerly case), (b) 06UTC 26 January, 2002 (easterly case), (c) 00UTC 3 June, 2002 (southerly case), and (d) 00UTC 21 February, 2002 (northerly case). From ECMWF operational analysis data. (Data is averaged over a three hour period from the times shown.)

the speed-up jet curving sharply to the left (partly due to low pressure system situated off the west coast of Greenland (see Fig. 6(a))), resulting in a strong, localised wind stress curl and downwelling.

6.4. Northerly Approach Flow

The strong speed-up jet evident around Cape Farewell and accelerating eastward, discussed in Section 5.4, consists of extremely cold, dry polar air and corresponds to regions of large negative surface heat flux. Figs. 8(d) and 9(d) show UM 4.5 and ECMWF modelled latent heat fluxes of up to -200 Wm^{-2}. Figs. 12(d) and 13(d) show a even larger sensible heat flux of up to -300 Wm^{-2}. Thus intense cooling of the ocean surface takes place through advection and evaporation, with resulting downwelling. (Additionally, there is a region of large negative surface heat flux off the southeastern coast from the cold, katabatic winds been funnelled off the ice sheet (see Fig. 8(d)).) Figs. 8(d) and 9(d) show the flow in the wake curving sharply to the left, resulting in strong wind stress curl and downwelling.

Table 5

Cloudiness and precipitation station reports for 12UTC 7 January, 2002 (westerly case)

Station WMO No.	Region of Greenland	Mean cloud cover (oktas)	Precip. (mm)
04220	mid west	8	2
04250	southwest	7.5	42
04260	further down, southwest	8	13.2
04272	extreme south-south-west	8	13.4
04390	extreme south	3.75	3.1
04360	southeast	2.63	7
04339	East	2.25	0.9

Table 6

Cloudiness and precipitation station reports for 12UTC 26 January, 2002 (easterly case)

Station WMO No.	Region of Greenland	Mean cloud cover (oktas)	Precip. (mm)
04220	mid west	4.75	0
04250	southwest	4.5	0
04272	extreme south-south-west	8	0
04390	extreme south	5.9	0
04360	southeast	4	0
04339	east	0.4	0

7. Cloudiness and Precipitation over Southern Greenland

HUNT *et al.*, (2004) confirmed theoretically that for stably stratified flow, in the areas where speed-up jets are shown (see Section 5) there are also changes to the inversion height. Applying their model to Greenland predicts that for westerly flows the air would sink as it crossed the southern tip of Greenland. And hence cloudiness and precipitation would decrease. Similarly, for easterly flows the air would rise as it crossed the southern tip of Greenland. And hence cloudiness and precipitation would increase. Note that their model does not take into account upstream conditions. In this section we examine observational evidence of these predictions.

7.1. Westerly Approach Flow

Table 5 shows observations from DMI coastal stations (averaged over the 24-hour period) for the westerly flow case study (7 January, 2002). The data show that cloud cover is considerably greater and amounts of precipitation higher on the west coast of Greenland than on the east coast. This follows because the synoptic flow was westerly and perhaps introduced moist air from the Labrador Sea. This is clearly seen as areas of bright white cloud around southwest Greenland on the infrared satellite images, especially at 15UTC (see Fig. 4(c)). By comparison the east coast appears comparatively clear on both the 05UTC and 15UTC images (see Figs. 4(b,c)).

7.2. Easterly Approach Flow

Table 6 shows observations from DMI coastal stations (averaged over the 24-hour period) for the easterly flow case study (26 January, 2002). The data show an overcast sky in the south-south-west and that the amount of cloud cover progressively increases southwards down the eastern side of Greenland. This is well seen in the infrared satellite image (see Fig. 5(b)). Especially note the high bright clouds around south and southwest of Greenland.

8. Discussion

8.1. Flow over Greenland

These studies show that typical air movements over Greenland do not generally correspond to the idealised conditions of uniform approach flow shown in Figs. 2 and 3, though such conditions also occasionally exist. Rather the typical upper level flow (at 500 mb) consists of synoptic eddies passing over the plateau. These change the topology of the streamlines, as seen in Fig. 8. But Fig. 3 shows that even if the large scale flow varies significantly over the bulk of the plateau, the characteristic features of the jet formation, with wind speeds of order 2–3 times that of the local

winds and a transverse scale of order of the Rossby deformation radius L_R, have an westerly or easterly component (HUNT *et al.*, 2001, 2004). Also evident are sharp gradients in the velocity perpendicular to the coastline and at the edges of the jet. The jets have a vertical scale of order $\sim$ 1000 m and are associated with rising/sinking air and the formation of clouds to the west and clearer air to the east of the tip of Greenland (HUNT *et al.*, 2004). Further theoretical and computational studies are necessary to understand how these synoptically driven surface flows are affected by non-uniform approach flows.

Another general feature of the surface flow is the generation of katabatic winds on the slopes caused by strong radiative longwave cooling over the ice sheet. Over the gently sloping central part of the ice sheet these winds are moderate. Winds accelerate towards the coastal margins where the topography steepens (e.g., see Fig. 8(d)). The strong katabatic flows are important to the energy balance of melting sea ice (e.g., BROMWICH *et al.*, 1996; KLEIN *et al.*, 2001). Over the ice sheet these are shown to be only moderately affected by the synoptic flow. However on the upwind side of Greenland they interact with the barrier jet (VAN DEN BROEKE and GALLÉE, 1996) and on the downside with large-scale wake eddies. But a general conceptual framework for the interaction has yet to be devised.

One of the purposes of this study is to see whether wind speed and direction measured at the coastal stations are representative of the broad-scale synoptic conditions (i.e., wind vectors over the sea shown by the UM 4.5 and ECMWF data). Coastal station winds are sometimes influenced by meso- and micro-scale meteorology (e.g., katabatic winds). However they are quite often, when taken together, broadly representative of the wider picture. On the other hand, it is clear that certain coastal stations are susceptible to particular local and mesoscale effects according to the prevailing synoptic situation.

In general the UM 4.5 modelled 10-m winds, computed using a horizontal resolution of 12 km, compared well both in magnitude and direction with the DMI and GC-Net station observations; as did the ECMWF operational analysis 10-m winds, though typically they were smaller than the observed wind speeds. Comparing the predicted UM 4.5 and ECMWF 10-m winds, the UM 4.5 data typically showed a stronger and more localised jet. Additionally it captured better the sharp gradients in the velocity perpendicular to the coastline and the interaction between the barrier jet and the katabatic winds. For accurate simulations of these flows, mesoscale models are necessary with horizontal resolutions of the order of 20 km or less.

8.2. Air-sea Interaction

The strong winds and cold temperatures of the low-level jets lead to enhanced heat loss in the ocean around southern Greenland. Typically latent heat fluxes were slightly greater than the sensible heat flux, but combined they typically contributed a strong heat flux of between -300 and -400 Wm^{-2}. Additionally the jets often curve

markedly to the left due to Coriolis, resulting in strong, localised wind stress curl. Due to Ekman motion this would create a cyclonic or divergent gyre in the ocean. Together the large sea-air heat flux and strong wind curl force oceanic downwelling (GILL, 1982). Recently PICKART *et al.*, (2003) showed that downwelling in the Irminger Sea (to the southeast of Greenland) was associated with the western Greenland tip jet (through strong wind stress curl and large air-sea heat flux). RENFREW *et al.*, (2002) observed deep convection in the western Labrador Sea due to a cooling heat flux comparable with results presented here.

However, the western tip jet is a relatively rare phenomenon (see Section 3.1). Results here suggest that downwelling associated with these jets might be associated at places other than the Irminger Sea and possibly more common than previously thought. Additionally, the wind-jets have implications for the movement of sea-ice, particularly in opening leads and polynyas and warming of the atmosphere (UOTILA, 2001; SMEDMAN, 2003). Note that ice movement is generally southward on the east coast of Greenland near the southern tip, corresponding to the airflow depicted in Fig. 3(b)(i).

In general the predicted UM 4.5 and ECMWF heat fluxes were of the same order of magnitude. However, UM 4.5 fluxes were typically confined to a narrower region, consistent with a more localised jet. UM 4.5 also typically predicted a stronger jet and therefore regions of stronger wind stress curl, suggesting it would predict greater, and possibly more accurate, downwelling (remember the ECMWF operational analysis data are generated using a substantially coarser $0.5^\circ \times 0.5^\circ$ grid). This indicates that perhaps improved parameterisation of air-sea coupling is required in numerical weather/climate prediction models.

8.3. Cloudiness and Precipitation

Are cloudiness and precipitation greater on the west coast of Greenland than on the east coast, in accordance with the model of HUNT *et al.*, (2004)? Data from the westerly and easterly case studies tentatively suggested this.

Measurements of cloud cover are prone to uncertainties as it is based on visual estimates by observers and partly missing records. Nevertheless from climatological records (CAPPELEN *et al.*, 2001) a pattern emerges of the east coast being relatively cloud-free compared with the west. The two cloudiest stations during 1961–1990 were 04250 (70% mean cloud cover (MCC)) and 04260 (71% MCC) in southwest Greenland, whereas 04320 in the northeast had only 50% MCC. 04390 near the southern tip of Greenland had an intermediate value of 63% MCC, and 04272 (also in the south) had 65% MCC. However, 04360 in the east had a relatively high value of 68% MCC. CAPPELEN *et al.*, (2001) suggest the southwest coast is about $\sim 10\%$ cloudier, on average, than the southeast coast but there are large local variations.

Regarding precipitation, this is also notoriously difficult to measure in the polar regions due to problems with blizzards and wind-blown snow. CAPPELEN *et al.*,

(2001) gives yearly precipitation amounts averaged over the period 1961–1990, showing that precipitation is highest at the southern stations, especially 04390 (extreme south; average of 2474 mm), followed by 04380 (southeast; 1535 mm), 04261 (extreme south-south-west; 1040 mm), 04360 (southeast; 984 mm), 04260 (south-south-west; 874 mm), and 04272 (extreme south-south-west; 858 mm). This suggests that precipitation is in fact greater in the southeast than the southwest, perhaps due to prevailing easterlies hitting the south-east coast of Greenland and being orographically forced. Thus further theoretical and computational studies are necessary to understand this aspect of Greenland's mesoscale climatology.

Acknowledgments

It is a pleasure to contribute to this volume in honour of Professor M. R. Singh, who stimulated much important research on geophysical fluid dynamics; Julian Hunt particularly benefited from his support and encouragement. We are grateful to the University of Dundee Satellite Receiving Station and NOAA for the satellite images. The MSLP analysis charts are copyright of the UK Met Office and were obtained from the Uni. Wetterzentrale Topkarten website. We are grateful to the British Atmospheric Data Centre for providing access to data from the European Centre for Medium-Range Weather Forecasts. Thanks to Paul Coles for the map of Greenland. Andrew Orr would like to thank Andy Shepard and Paul Taylor. This work was supported by grants from NERC to the Depts. of Space & Climate Physics and Mathematics at University College London. Julian Hunt is grateful to the Mechanical and Aerospace Engineering Department, Cornell University where he is the Mary B. Upson visiting Professor.

References

Baines, P. G., *Topographic Effects in Stratified Flows* (Cambridge University Press, UK, 1995).

Blumen, W. (Editor), *Atmospheric Processes over Complex Terrain* (Meteorological Monographs, Ame. Meteorol. Soc., *23*, 1990).

Boyer, D. L. and Chen, R. (1987), *Laboratory Simulation of Mountain Effects on Large-scale Atmospheric Motion Systems: The Rocky Mountains*, J. Atmos. Sci. *44*, 100–123.

Boyer, D. L. and Davies, P. A. (2000), *Laboratory Studies of Orographic Effects in Rotating and Stratified Flows*, Annu. Rev. Fluid Mech. *32*, 165–202.

Bromwich, D. H., Du, Y., and Hines, K. M. (1996), *Wintertime Surface Winds over the Greenland Ice Sheet*, Mon. Wea. Rev. *124*, 1941–1947.

Capon, R. (2003), *Wind Speed-up in the Dover Straits with the Met Office New Dynamics Model*, Meteorol. Appl. *10*, 229–237.

Cappelen, J., Jorgensen, B. V., Laursen, E. V., Stannius, L. S., and Thomsen, R. S., *The Observed Climate of Greenland, 1958–99, with Climatological Standard Normals, 1961–90*. (Tech. Rpt. 00-18, Danish Meteorol. Institute, Copenhagen, Denmark, 2001).

CLARK, P. A. and HOPWOOD, W. P. (2001), *One-dimensional Site-specific Forecasting of Radiation Fog. Part 1: Model Formulation and Idealised Sensitivity Studies*, Meteorol. Appl. *8*, 279–286.

COLEMAN, A. and DAVEY, M. (1999), *Prediction of Summer Temperature, Rainfall and Pressure in Europe from Proceeding Winter North Atlantic Ocean Temperature*, Int. J. Climatol. *19*, 513–536.

CONNOLLEY, W. M. and CATTLE, H. (1994), *The Antarctic Climate of the UKMO Unified Model*, Antarctic Science *6*, 115–122.

CULLEN, M. J. P. (1993), *The Unified Forecast/Climate Model*, The Meteorol. Mag. *122*, 81–94.

DING, L. and STREET, R. L. (2003), *Numerical Study of the Wake Structure behind a Three-dimensional Hill*, J. Atmos. Sci. *60*, 1678–1690.

DOYLE, J. D. and SHAPIRO, M. A. (1999), *Flow Response to Large-scale Topography: The Greenland Tip Jet*, Tellus *51A*, 728–748.

GILL, A. E., *Atmosphere-Ocean Dynamics* (Academic Press, London, UK, 1982).

GLOVER, R. (1999), *Influence of Spatial Resolution and Treatment of Orography on GCM Estimates of the Surface Mass Balance of the Greenland Ice Sheet*, J. Climate *12*, 551–563.

HANNA, E. and CAPPELEN, J. (2003), *Recent Cooling in Coastal Southern Greenland and Relation with the North Atlantic Oscillation*, Geophys. Res. Lett. *30*, 1132.

HOZUMI, Y. and UEDA, H. (2005), *Numerical Study on Vortices in the Middle Layer of Flow around a Large Mountain under Rotating Stratified Conditions*, Pure. Appl Geophys. 162 (10) this issue.

HUNT, J. C. R., ABELL, C. J., PETERKA, J. A., and WOO, H. G. C. (1978), *Kinematic Studies of the Flow around Free or Surface-mounted Obstacles: Applying Topology to Flow Visualisation*, J. Fluid Mech. *86*, 179–200.

HUNT, J. C. R. and SNYDER, W. H. (1980), *Experiments on Stably Stratified Flow over a Model Three-dimensional Hill*, J. Fluid Mech. *96*, 671–704.

HUNT, J. C. R., FENG, Y., LINDEN, P. F., GREENSLADE, M. D., and MOBBS, S. D. (1997), *Low Froude Number Stable Flows past Mountains*, Il Nuovo Climento *20C*, 261–272.

HUNT, J. C. R., ÓLAFSSON, H., and BOUGEAULT, P. (2001), *Coriolis Effects on Orographic and Mesoscale Flows*, Q. J. Roy. Met. Soc. *127*, 601–633.

HUNT, J. C. R., ORR, A., ROTTMAN, J. W., and CAPON, R. (2004), *Coriolis effects in mesoscale flows with sharp changes in surface conditions*, Q. J. Roy. Met. Soc., *130*, 2703–2731.

JORGENSEN, P.V. and LAURSEN, E. V., *DMI Monthly Climate Data Collection 1860–2002, Denmark, Faroe Island and Greenland* (An Update of: NACD, REWARD, NORDKLIM and NARP datasets Version 1. Tech. Report 03-26, Danish Meteorological Institute, Copenhagen, Denmark, 2003).

KLEIN, T., HEINEMANN, G., and GROSS, P. (2001), *Simulation of the Katabatic Flow near the Greenland Ice Margin using a High-resolution Nonhydrostatic Model*, Meteorologische Zeitschrift *10*, 221–339.

KLEIN, T. and HEINEMANN, G. (2002), *Interaction of Katabatic Winds and Mesoscyclones near the Eastern Coast of Greenland*, Meteorol. Appl. *9*, 407–422.

LOTT, F., and MILLER, M. J. (1997), *A New Subgrid-scale Orographic Drag Parameterization: Its Formulation and Testing*, Q. J. Roy. Met. Soc. *123*, 101–127.

MEESTERS, A. (1994), *Dependence of the Energy Balance of the Greenland Ice Sheet on Climate Change: Influence of Katabatic Wind and Tundra*, Q. J. Roy. Met. Soc. *120*, 491–517.

MERKINE, L. O. (1975), *Steady Finite-amplitude Baroclinic Flow over Long Topography in a Rotating, Stratified Atmosphere*, J. Atmos. Sci. *32*, 1881.

NEWLEY, T. M. J., PEARSON, H. J., and HUNT, J. C. R. (1991), *Stably Stratified Rotating Flow through a Group of Obstacles*, Geophys. Astrophys. Fluid Dyn. *58*, 147–171.

ÓLAFSSON, H., and BOUGEAULT, P. (1996), *Non-linear Flow past an Elliptic Mountain Ridge*, J. Atmos. Sci. *53*, 2465–2489.

ÓLAFSSON, H. and BOUGEAULT, P. (1997), *The Effect of Rotation and Surface Friction on Orographic Drag*, J. Atmos. Sci. *54*, 193–210.

ÓLAFSSON, H. (2000), *The Impact of Flow Regimes on Asymmetry of Orographic Drag at Moderate and Low Rossby Numbers*, Tellus *52A*, 365–379.

PETERSEN, G. N., ÓLAFSSON, H., and KRISTJÁNSSON, J. E. (2003), *Flow in the Lee of Idealized Mountains and Greenland*, J. Atmos. Sci. *60*, 2183–2195.

PIERREHUMBERT, R. T. and WYMAN, B. (1985), *Upstream Effects of Mesoscale Mountains*, J. Atmos. Sci. *42*, 977–1003.

PICKART, R. S., SPALL, M. A., RIBERGAARD, M. H., MOORE, G. W. K., and MILLIFF, R. F. (2003), *Deep convection in the Irminger Sea Forced by the Greenland Tip Jet*, Nature *424*, 152–156.

PUTNINS, P., *The climate of Greenland*. In *World Survey of Climatology Volume 14: Climates of the Polar Regions* (eds. Orvig, S.; Landsberg, H. E.) (Elsevier Publishing Company, New York, 1970) pp. 3–128.

RASMUSSEN, L. (1989), *Greenland Winds and Satellite Imagery*, VEJRET (in English) (ed. Nilsen, N. W.), Danish Meteorol. Soc., pp. 32–37.

RENFREW, I. A., MOORE, G. W. K., GUEST, P. S., BUMPKE, K. A. (2002), *A Comparison of Surface-layer Heat Flux and Surface Momentum Flux Observations over the Labrador Sea with ECMWF and NCEP Reanalyses*, J. Phys. Oceanogr. *32*, 383–400.

SCORER, R. S. (1988), *Sunny Greenland*, Q. J. Roy. Met. Soc. *114*, 3–29.

SMEDMAN, A. S., HÖGSTRÖm, U., and HUNT, J. C. R. (2003), *Effects of Shear Sheltering in a Stable Atmospheric Boundary Layer with Strong Shear*, Q. J. Roy. Met. Soc. *130*, 31–50.

SMOLARKIEWICZ, P. K. and ROTUNNO, R. (1989), *Low Froude Number Flow past Three-dimensional Obstacles. Part I: Baroclinically Generated Lee Vortices*, J. Atmos. Sci. *46*, 1154–1164.

SNYDER, W. H., THOMPSON, R. S., ESKRIDGE, R. E., LAWSON, R. E., CASTRO, I. P., LEE, J. T., HUNT, J. C. R., and OGAWA, Y. (1985), *The Structure of Strongly Stratified Flow over Hills: Dividing-streamline Concept*, J. Fluid Mech. *152*, 249–288.

STAMMERJOHN, S. E., DRINKWATER, M. R., SMITH, R. C., and LIU, X. (2003), *Ice-atmosphere Interactions during Sea-ice Advance and Retreat in the Western Antarctic Peninsula Region*, J. Geophys. Res. *108*, 3329.

STEFFEN, K. and BOX, J. (2001), *Surface Climatology of the Greenland Ice Sheet: Greenland Climate Network 1995–1999*, J. Geophys. Res. *106*, 33,951–33,964.

UOTILA, J. (2001), *Observed and Modelled Sea-ice Drift Response to Wind Forcing in the Northern Baltic Sea*, Tellus *53A*, 112–128.

VAN DEN BROEKE, M. R. and GALLÉE, H. (1996), *Observation and Simulation of Barrier Winds at the Western Margin of the Greenland Ice Sheet*, Q. J. Roy. Met. Soc. *122*, 1365–1383.

VOSPER, S. B., CASTRO, I. P., SNYDER, W. H., and MOBBS, S. D. (1999), *Experimental Studies of Strongly Stratified Flow past Three-dimensional Orography*, J. Fluid Mech. *390*, 223–249.

WOOD, N., and MASON, P. (1993), *The Pressure Force Induced by Neutral, Turbulent Flow over Hills*, Q. J. Roy. Met. Soc. *119*, 1233–1267.

(Received January 20, 2004, accepted April 12, 2004)